Smart Agricultural Technology 10 (2025) 100756

Contents lists available at ScienceDirect

Smart Agricultural Technology

journal homepage: www.journals.elsevier.com/smart-agricultural-technology

Identifying phenotypic markers explaining positive sorghum response to sowing density using 3D-imaging

Wenli Xue [a,b], Ewaut Kissel [b], András Tóth [b], Raphael Pilloni [c,d], Vincent Vadez [a,e,*]

[a] IRD (Institute for Research and Development, University of Montpellier, DIADE Research Unit, 911 Av. Agropolis, 34394 Montpellier, France
[b] Phenospex B.V., Jan Campertstraat 11, 6416 SG Heerlen, the Netherlands
[c] CIRAD (Centre International de Recherche Agronomique pour le Developpement), AIDA Research Unit, University of Montpellier, Montpellier, France
[d] CIRAD, UPR AIDA, F-97743 Saint-Denis, La Réunion, France
[e] Centre d'Étude Régional pour l'Amélioration de l'Adaptation à la Sécheresse (CERAAS), Thiès, Sénégal

ARTICLE INFO

Keywords:
3d-imaging assisted phenotyping
Light penetration
Photosynthesis
Sowing density
Spearman correlation
Principal component analysis
ANOVA

ABSTRACT

Sorghum genotypes vary in their response to higher sowing density, but the traits explaining these variations are unknown. In the present study, a 3D-imaging based approach identified the phenotypic traits responsible for the genetic variation in sorghum's response to high sowing density. Twenty sorghum genotypes, some varying in their response to density, were grown and 3D-images were collected weekly between weeks 4–6. From these images, 80 phenotypic traits, including 33 architectural and 47 multispectral, were extracted. The within-genotype means of these 80 traits, and two indicators of the sowing density response (Biomass ratio (Br) and Transpiration ratio (Tr)), measured in a previous study with 13 common genotypes, were used in a Spearman correlation analysis. Seventeen and four traits were strongly correlated with Br and Tr, respectively. The majority of these traits, predominantly architectural, strongly suggest that, under high sowing density, a fuller light interception, having more leaf area in the lower canopy, lead to a larger Br, while more vertically aligned leaves favour larger Tr values, which related to higher water use efficiency in another study. Furthermore, a Principal Component Analysis (PCA) indicated traits contributing to better photosynthesis could be used to estimate Br. Similarly, a combination of traits relating to leaf angle were good indicators of the genetic variation in Tr values. These results provide insights about the strategies some sorghum genotypes have developed to thrive under higher sowing density and that could be used as biomarkers for the breeding of density-resistant cultivars.

1. Introduction

The unprecedented drastic changes, e.g., frequent extreme weather events, rapidly growing population, and consumption needs on both the global and local scales, have imposed an enormous strain on food supply security in developing countries. To cope with such a challenge, increasing yields of staple crops such as sorghum, which feeds 500 million people in 30 countries (mostly in underdeveloped regions), is needed [1,2]. Sorghum is often cultivated in poor soils and at low sowing density, a hurdle to be overcome to increase its productivity with limited resources. Certain sorghum genotypes respond positively to an increase in sowing density, but not all, especially under conditions of high evaporative demand [3]. These promising results show that it is possible to increase the productivity of sorghum with existing cultivars, and that the genotypic variability in its response to density opens the possibility to breed novel cultivars more adapted to high density stands.

The genotypic variations in density response could be attributed to differences in canopy architecture traits, such as leaf area and leaf angle [4–6]. The leaf area of a plant determines the surface availability to intercept light and consequently impacts yield [5]. The leaf angle or the orientation of leaves across the canopy affects how light is distributed across leaves that are positioned at different heights; hence it affects the ability of light interception of a plant. For instance, studies have shown that vertically aligned leaves allow light to penetrate deeper into the canopy, which might theoretically lead to an increase in photosynthetic activities and yields [4,7–10]. Furthermore, a recent research in maize has revealed that the leaf area distribution along the vertical axis has been indirectly selected in the past 65 years and has favoured a deeper

* Corresponding author: IRD (Institute for Research and Development, University of Montpellier, DIADE Research Unit, 911 Av. Agropolis, 34394 Montpellier, France
E-mail address: vincent.vadez@ird.fr (V. Vadez).

https://doi.org/10.1016/j.atech.2024.100756
Received 4 November 2024; Received in revised form 23 December 2024; Accepted 24 December 2024
Available online 27 December 2024

light distribution in the canopy, leading to a higher light interception [11]. This might also explain that the planting density of maize has increased three-fold over the last century. However, the latter studies were either theoretical studies and/or simulations of the effect of these traits on photosynthetic activity or light interception using virtual canopies. For example, there was variation in leaf angle among maize genotypes, and those with upright leaf angle where better able to intercept radiation [9]. While the variation in angles was physically measured, its effect on light interception was assessed from a virtual canopy. In addition, these studies (except [10]) have not been followed by field-based experimentation to test the value of these architectural trait differences.

Genotypic variations in the degree of response to an increased sowing density have been found in sorghum [3] in a small panel of cultivars. Several traits have been suggested in other species that could explain the propensity to respond positively to an increase in sowing density, on the basis of simulations. A larger screening of potential donor parents in sorghum and a better understanding of physiological traits responsible for this response is necessary. However, the link between a positive response to density in the field and physiological traits explaining this response has not been established in sorghum. Indeed, earlier work in sorghum [10] only showed evidence of a better light interception in virtual canopies and between two genotypes contrasting in their leaf inclination angles, and no test on the response to planting density has been done. In addition, earlier work in sorghum has only focused on leaf angle [10], whereas other traits have been identified in other species, like the leaf distribution along the vertical axis in maize [11]. Therefore, a systematic and comprehensive search of the phenotypic features that are tightly correlated to differences in density responses among genotypes is necessary. Part of the reason why this has not been done in the past is that traits responsible for a positive response to density are traits that deal with light distribution in the canopy. These architectural traits, operating in the 3-dimensional (3D) space are hard to measure consistently. This is where sensor-based phenotyping, which has the advantage of generating a large number of (complex) traits within a short period of time, is considered as the suitable tool for such task [12–17].

The use of sensor-based approach to extract traits related to plant growth, development, yield and tolerance to biotic and abiotic stresses has become a promising asset for breeding [14,18–24]. There are various types of sensor-based plant phenotyping and the majority of the reported methods are quantification of morphological, architecture, texture and colour-based traits from 2D images [20,23,24,25–27]. 2D-imaging has difficulties providing reliable and sufficient information of 3D structures of plants, e.g. self-occlusion and curvature of stem and leaves, because of parallax and information loss when projecting 3D structures onto a 2D plane. For instance, the internode distance of curved plants cannot be accurately estimated from sequences of 2D images using multiple viewing-angles, because the curvature of the stem between two nodes is difficult to be quantified in 2D space [24].

A relatively novel type is based on 3D-imaging, which has the advantage of obviating those difficulties and capturing the 3D structures of plants, which enables an accurate estimation of traits and thus facilitates reliable analysis. In this study, a 3D scanner, referred to as PlantEye from Phenospex.BV, was used to generate data of plants including both multispectral and structural traits. Those traits together gave an accurate and comprehensive representative of a plant. Furthermore, 3D images have the advantage of allowing realistic estimations of structural traits. For instance, leaf area derived from 3D images was calculated taking the curvature of leaves into account, which was often overlooked in 2D-image based methods due to its 2D nature [25].

However, a missing step here is to have a real-world assessment to test if any of these traits could be related to field-based difference in crop performance, and this is a big gap in many of the reported studies that rely on modelling. In our case, while a first step was to develop the capacity to phenotype for a series of diverse traits that represent the 3D architecture of a crop canopy, the next step was to test whether any of these traits correlates with assessment of the density response in the real world. Therefore, the innovation we propose in this work is to take the technical advantage of 3D-imaging to help us decipher and identify the traits involved in the 3D architecture of plants. Having seen above the importance of planting density to boost sorghum productivity, we would then like to test the putative link between these 3D traits and the propensity of a genotype to respond to an increase in the sowing density. Here, two biological traits of importance for plant productivity under high density were targeted: (i) the ratio of the biomass under high density to that under low density (i.e. biomass ratio, Br), which measures the capacity to respond positively to an increase planting density [3]; (ii) the capacity to increase canopy transpiration under high evaporative demand [28]. Regarding this second trait, it has been recently

Table 1
Description of correlated traits with Br and Tr from Test 3, along with their category (canopy or spectral type) and brief descriptions.

Traits names	Category	Correlation	Brief description
voxel_ratio_'n'	canopy	Br	The percentage of voxel volume of the n^{th} section from the top (out of ten sections) over the total voxel volume. This voxel ratio then expresses the distribution of voxels (unit elements of the leaf area) in the vertical axis
hull_coverage (%)	canopy	Br	The hull being the projected contour of the plant on the ground, and the hull area the area of that shape, the percentage of the hull area occupied by the plant's 2D projection represents the proportion of the plant's projection that is covered by its leaves. A large value indicates less overlapped leaves and/or more upright leaves along the stem
voxel_kurtosis	canopy	Br	The distribution of the leaves along the plant's stem, which is calculated by the kurtosis of voxel volume distribution. A large kurtosis value indicates voxels are not uniformly distributed along the vertical axis, for instance a plant with a relative large proportion of the voxels in the bottom part along the vertical axis
lightness_adj	canopy	Br	The depth of light penetration is measured as the difference between the heights of the top and bottom voxels detected by the scanner and divided by the plant height
average_surface_angle	canopy	Tr	Represents the average angle of the triangles relative to the vertical axis. It is calculated as the weighted average of all angles formed by the normals of every face in the plant mesh. A high value reflects plants with more prostrated leaves whereas a small value reflects more erected leaves
leaf_inclination	canopy	Tr	The average orientation of a plant's leaves, indicating how upright or angled they are. It is calculated by dividing the plant's total leaf area by the projected leaf area
hull_packed	canopy	Tr	The percentage of hull area within its circumference
psri_[-inf:−1]	Spectral	Tr	The percentage of 3D points in a specific PSRI range compared to the total number of 3D points

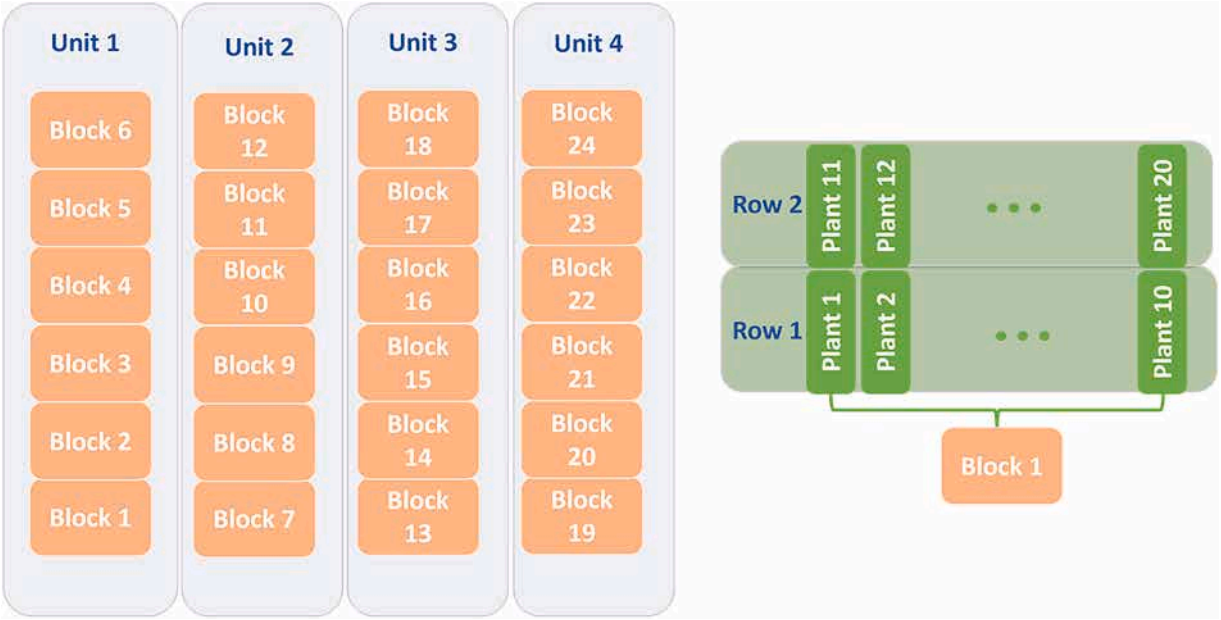

Fig. 1. Left: Illustration of blocks and units; Right: The arrangement of plants in a block using block 1 as an example.

shown that sorghum genotypes that most increased productivity under high density also increased water use efficiency (WUE, i.e. biomass/water transpired) [3]. In addition, it was shown that in conditions of high evaporative demand, sorghum genotypes with highest WUE were those displaying the strongest transpiration response to an increase in the evaporative demand [3,28]. Hence, the second biological trait we target is also inherently related to the capacity of genotypes to respond to high sowing density.

Therefore, the present study aims at 1) identifying traits that can be correlated to sorghum's known responses to sowing density and transpiration under high evaporative demand and 2) investigating the feasibility of using a combination of these traits to distinguish genotypes of various levels of density response. The authors hope to bring more biological insights about how some sorghum genotypes thrive under a high sowing density environment, via the manipulation of certain phenotypic features. These insights can potentially pave a path for breeding high density-adapted cultivars.

2. Materials and methods

2.1. Experiment settings and procedure

480 plants from 20 genotypes of sorghum (24 plants per genotype) were grown in individual 7 L pots (1 seed per pot). The plants were positioned in a 2D-coordinate system with 10 columns and 48 rows, and they were labelled using integers from 1 to 480 (the list of genotypes used for each plant can be found in the Suppl. Table 1).

Each 2 rows formed a block. The blocks were marked in a number sequence from 1 to 24. Every block contained 20 plants (1 per genotype) and the locations of these plants within the block were randomized. The glasshouse was divided into 4 units based on the geographic layout, i.e. all units were separated from each other by existing pathways in the greenhouse. Every unit consisted of 6 blocks except unit 4 that contained 4 blocks. The 18 blocks in the first 3 units were used for data analysis and the 4 blocks in unit 4 were designed as backup. The back up plants were only used to replace abnormal ones from non-backup blocks (unit 1—3). The replacement befell within genotype, while a plant from non-backup blocks showed visible abnormal signs, e.g., discoloured, or pale leaves from possible growth defect. A substitute plant should comply with 2 criteria: 1) same genotype as the original plant and 2) comparable phenotypic appearance with the original plant, e.g., number of tillers and leaves. The arrangement of the plants can be seen in Fig. 1.

The plants grew for 3 weeks, from 13th February to 6th March 2023 in a glasshouse of the Institute of Research for Development (IRD) in Montpellier, France. Afterwards, the 3D scanning and manual measurement started, which took place once per week between 13th and 27th March 2023 in 3 consecutive tests, namely test 1, 2 and 3.

2.2. Manual measurements

Manual measurements included: 1) numbers of visible collars and 2) node height. A visible collar was defined as a light-coloured scar on the stem where leaves emerged [24]. The distance between soil surface and a visible collar was referred to as node height. The numbers of visible collars of each plant were manually measured and recorded. The main purpose of the manual measurements was to anchor a scanning date to temperature-related number of collars and corresponding node height rather than to a calendar date.

2.3. 3D image acquisition

3D images of plants were captured using a 3D-scanner, PlantEye F500 (Phenospex B.V.), which has a span of 80 × 194 cm. That span allowed plants to be scanned in pairs, with high resolution scans and no overlap between plants and no leaf falling out of range. Plants were scanned following the order based on their labels. For instance, plants labelled as 5 and 6 were scanned at the same time.

2.4. Data pre-processing

3D raw images were inspected visually first and then processed to generate 63 default quantitative traits, using the in-house software from PlantEye F500. Afterwards, 17 additional traits, related to 3D canopy architecture, were also designed, coded, and extracted from the raw image data. In total, 80 features (33 canopy and 47 multispectral traits) were derived from every 3D plant image weekly and their description can be found in the supplemental document (Suppl. Table 2).

Features acquired from both manual measurements and 3D data were analysed statistically (e.g., statistical description, box and whisker plot, histogram) to evaluate genotypic variation and phenotypic ranges

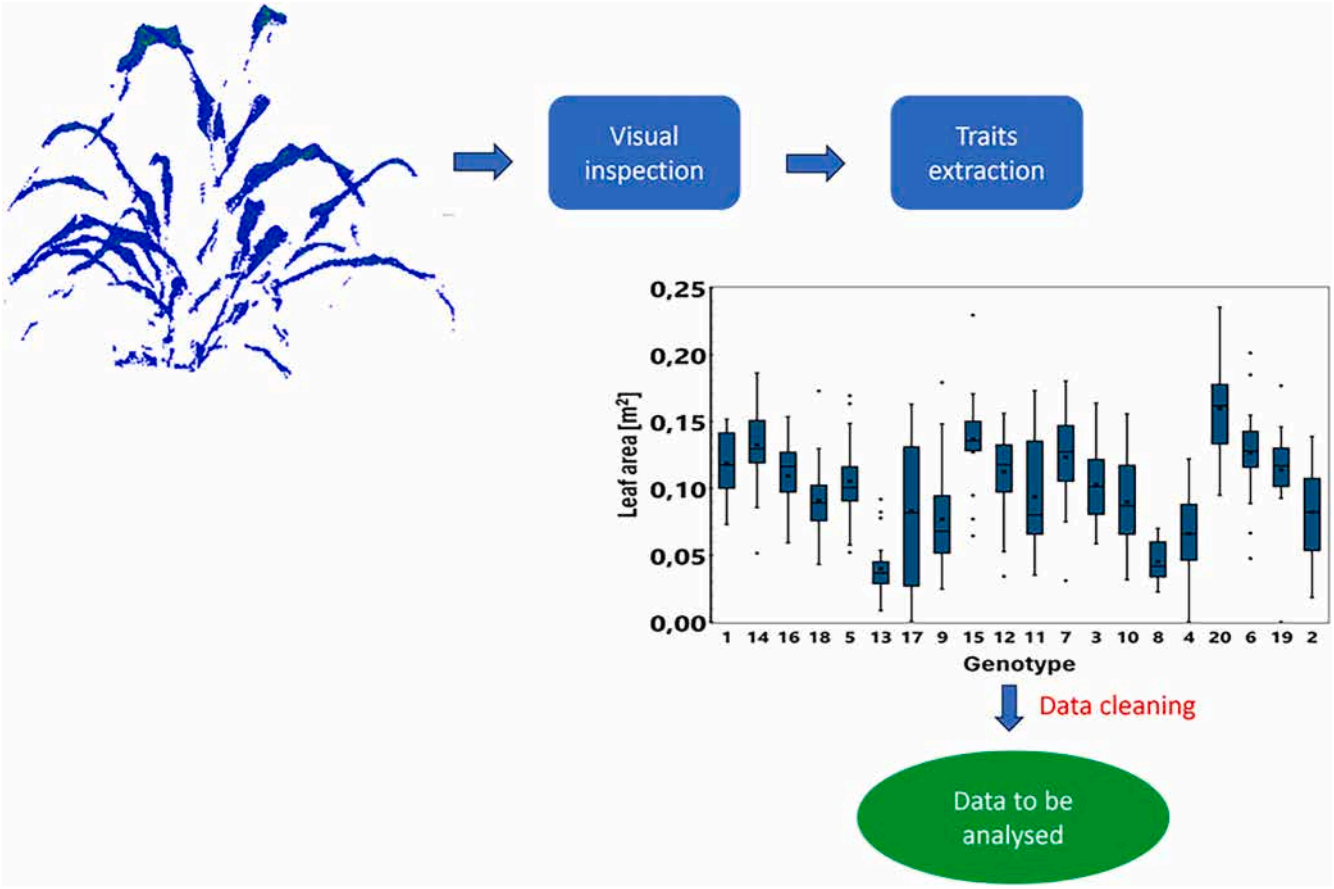

Fig. 2. Block scheme of data pre-processing. The boxplot of leaf area [mm^2] distribution in test 3 from each genotype is displayed as an example, and potential outliers detected, e.g., circled, are further evaluated to determine whether or not they should be removed from data analysis.

for each trait. A plant with 1 or more traits beyond whiskers in the boxplots was considered as a potential outlier, which was further evaluated and removed, if justified from the evaluation. The block scheme of data pre-processing is depicted in Fig. 2.

2.5. *Description of the indicators of the density response*

Biomass Ratio (Br) and Transpiration Ratio (Tr) were acquired from a reported study (Chapter 3.1 in Pilloni, 2022) – and these values are used here in the correlation analysis (Section 2.6 below) - aiming at identifying genotypic variation in the response of sorghum genotypes to an increase in planting density. In short, in this earlier work plants were cultivated until maturity in an outdoors condition lysimeter platform at the Bambey station in Senegal, so that there was no control over the temperature, relative humidity and solar radiation. Lysimeters are tubes of 25 cm diameter and 1.5 m length, filled with a sandy soil from the station. They were set up in trenches to avoid direct solar radiation and heating of the tubes, and put next to one another at a density of 8 tubes m^{-2}, so that plants grown in these lysimeters would rapidly form a crop canopy and mimic a real field environment [29,30]. The trial included 25 genotypes, 13 in common with the current work. Two density treatments were applied, either 8 or 16 plant m^{-2}. This work was set in the broader context of attempts to intensify the production of important staple grains like sorghum, by increasing its planting density, with very promising results [3]. The first of these density treatments correspond to the one currently used in experimental trials and the second one was hypothesized to boost biomass production. In the high density treatment, one replication consisted of four tubes planted each with one plant per tube. In the low density treatment, one replication consisted of four tubes also, with only two tubes with one plant per tube, the two other tubes remaining empty. Each genotype was replicated four times. Transpiration was measured in the lysimeters by weekly weighings of lysimeters, transpiration being the weight difference between two weighings plus water added in between weighings. After harvest, water use efficiency (WUE) was calculated as the ratio of the aboveground biomass divided by the cumulated transpiration.

In this work, the biomass ratio (Br) was calculated as:

Br = biomass in high density / biomass in low density

This ratio was a proxy to assess the propensity of a given genotype to respond to higher sowing density, with high Br ratio values reflecting large biomass increases under high density relative to that in low density. Details are available in ([28], Chapter 3.1).

Then, the transpiration response slope (Tr) was defined as the slope of the regression line that fitted the response of plant's transpiration to an increase in the evaporative demand. The latter was measured by the Penman-Monteith equation (ETref) [31,32] which is a meteorologic variable whose main factors are solar radiation, temperature, relative humidity (%) and wind. High ETref lead to high transpiration values. Transpiration values were obtained from the weighing of the lysimeters (see above), and were plotted against the cumulated ETref for each corresponding window. Transpiration response slopes (Tr) were then obtained from linear models fitting these scatter diagrams. Our interest in Tr and its linkage to the density response came from the following two major findings in Pilloni's work [28]: (i) Genotypes with high transpiration response slope values had higher water use efficiency (WUE, i.e. biomass/water transpired) in sorghum under high evaporative demand [28]; (ii) Genotypes showing the largest biomass response to a high sowing density were also those showing the largest WUE increase under high density, both in pearl millet [33] and sorghum [3], under high evaporative demand. So that the Tr trait was a physiological trait that

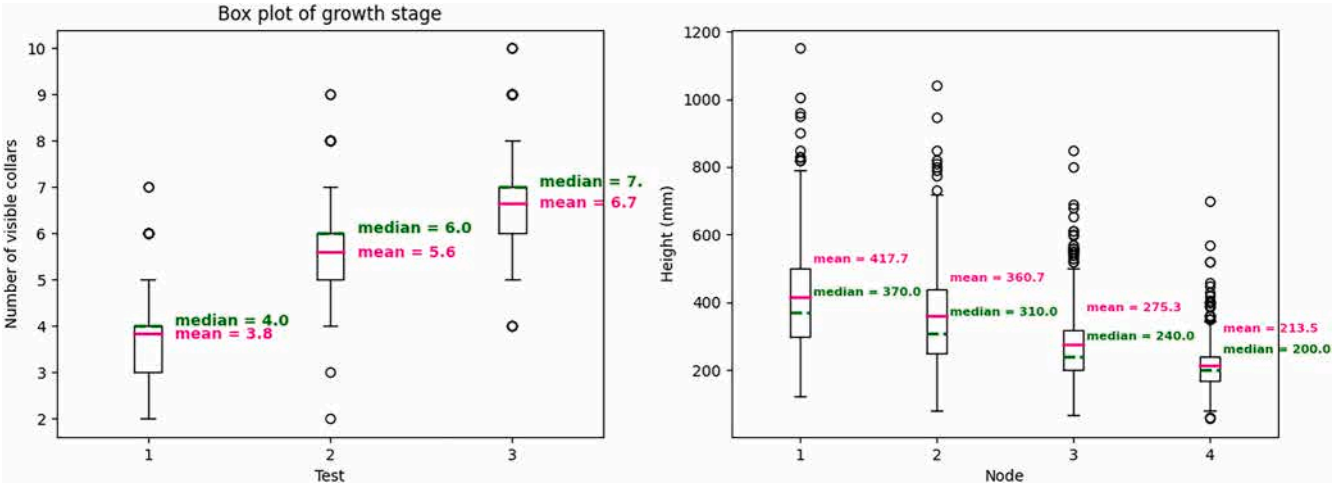

Fig. 3. Left: distribution of growth stages at the time of Scanning; Right: Distribution of node heights from top 4 nodes of each plant, measured in test 3.

was positively and indirectly related to the response to density, via its effect on WUE. Therefore, both Tr and Br were used as indicators to reflect the propensity for a positive response to an increased sowing density. We used the mean values of the Br ratio and of the Tr slopes from Pilloni's work [28], for those genotypes (13) that were common with the present work, in the Spearman correlation described thereafter.

2.6. Identification 3D traits correlated to sowing density response indicators

Following data pre-processing, a Spearman correlation test was performed to evaluate the monotonic relationship between each trait generated from 3D plant images with the two density indicators described above.

The within-genotype averages of all traits measured by the F500 scanner, along with Tr and Br, from selected genotypes (13 in common between the current study and the previous from Vadez et al. [28]) were used in this Spearman test and the subsequent data analysis. Features were screened based on the statistical significance testing of Spearman correlation ($\alpha = 0.05$). The strength of the correlation is determined by correlation coefficient and the further away the coefficient value from 0, the stronger the correlation is. After the test, the features with strong correlations with Br or Tr (Spearman correlation coefficient $r > 0.7$), as well as p values lower than α, were used for the subsequent PCA analysis.

2.7. Genotype discrimination

The features strongly correlated to Tr and Br were further evaluated using Principal Component Analysis (PCA), to explore the possibility of distinguishing genotypes with low and high Tr or Br responses, by using a combination of those selected traits.

The traits that had the most impact on Principal Component 1 (PC1) and PC2 were further evaluated via a One-way ANOVA ($\alpha = 0.05$), using genotype as the factor. After the ANOVA, a post-hoc Tukey analysis was performed, to confirm that significant genotypic variations exist among genotypes for those traits. The Tukey analysis was selected, as it is commonly used to evaluate full pair-wise comparison (between genotypes), instead of specific pairs (e.g., Bonferroni test), and each genotype has approximately equal number of samples. The normality of the selected feature data was evaluated via their probability plots versus normal distribution (see Fig. S1 in the supplementary document for details). The homogeneity of the variance was investigated by plotting residues as functions of fitted values (see Fig. S2 in the supplementary document for details).

3. Results and discussions

3.1. Experiment overview

Manual and 3D-image measurements of all 400 non-backup plants have been conducted in three consecutive tests, namely Test 1, 2 and 3, with 1 week between each other. After Test 1, 46 out of 400 plants were replaced using the plants from the backup blocks, due to visible discoloration. Thenceforward no plant was substituted, so that plants used in Test 2 and 3 were the same.

3.2. Growth stage of plants in each test

The number of visible collars and the heights of nodes of a plant are dependent on its development and growth stages. Fig. 3 (left) shows the evolution of growth stages in Test 1—3, which is characterised by the numbers of visible collars [25], manually measured during each Test. For instance, a plant with 5 visible collars is designated to be at growth stage vegetative 5 (V5). The medium growth stage of Test 1 (week 1, March 13th), 2 (week 2, March 20th) and 3 (week 3, March 27th) was V4, V6 and V7, respectively, while the average numbers of visible collars collected during each test was 3.8, 5.6 and 6.7, respectively. The right plot of Fig. 3 displays the node heights from the top 4 nodes, from all plants, in Test 3 to provide an overview of the sizes of plants during scanning in this test.

3.3. Data pre-processing

The manual measurement data has been visually inspected first and no missing data or extreme values, i.e., values deviating from the rest of the data by one order of magnitude, have been observed. Furthermore, the raw images showed that the plants were accurately captured with little to no occlusion and disruption e.g., turnover pots, broken stems and leaves.

The distribution of each trait, within the same genotype, was evaluated and visualised in boxplots (see the boxplot of leaf areas in Fig. 2 for one example). A plant with 1 or more traits beyond whiskers in the boxplots was considered as a potential outlier. The raw images of identified potential outlier plants have been visually evaluated and no plant was removed after the assessment. Meanwhile, 6 images (4 from Test 1 and 2 from Test 3) failed to generate traits and have been consequently removed from further analysis. In the end, the number of plants remaining after pre-processing was 396, 400 and 398 for Test 1, 2 and 3, respectively.

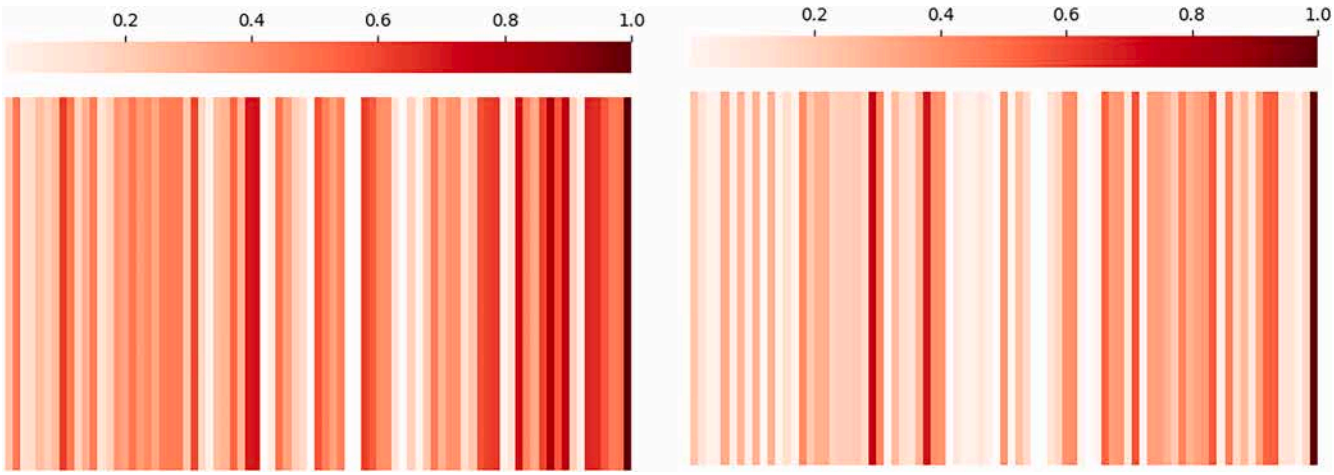

Fig. 4. Heatmap of Spearman correlation coefficients r of each pair of individual traits with Br (left) and Tr (right). The colour of each column represents the absolute value of r between each individual trait with either Br or Tr.

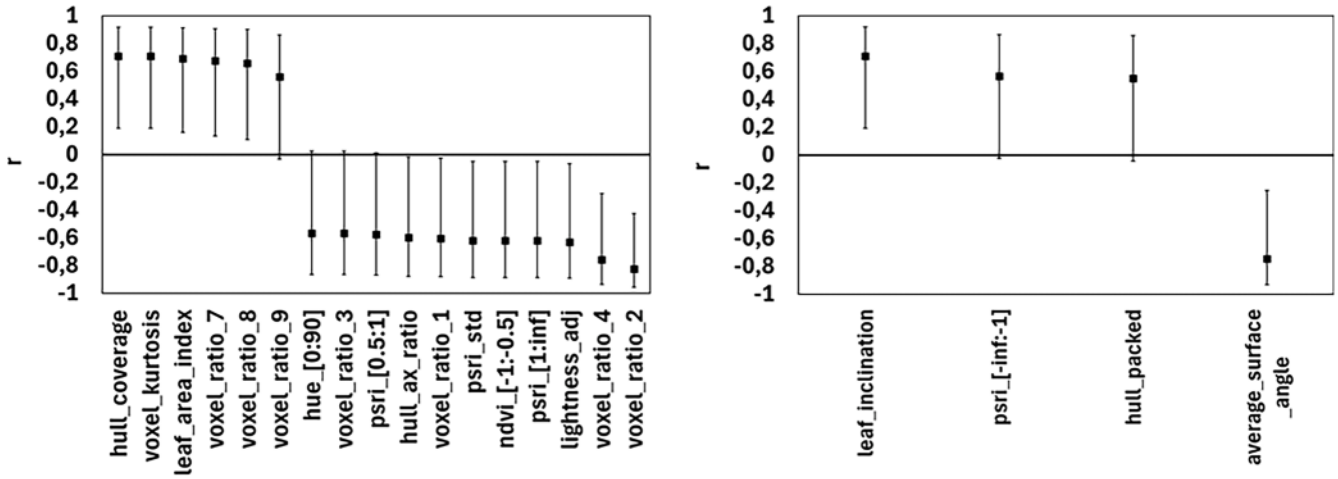

Fig. 5. Spearman coefficients r and their 95 % confidence intervals (CIs) of correlated traits with Br (left) and Tr (right) from Test 3.

3.4. Identification of 3D traits correlated to sowing density indicators

Among the genotypes that were tested, 13 out of 20 genotypes had corresponding Tr and Br values from the earlier work (Chapter 3.1 in Pilloni [28]), and the monotonic correlation test was conducted using data from those 13 genotypes. The correlation between individual traits from Test 3 with Br and Tr varied (Fig. 4). This figure summarizes the Spearman correlation coefficients of each trait with Br (left graph) and Tr (right graph) in the format of heat maps. Traits with darker colour, indicating a higher absolute *r* value, can potentially be those phenotypical features correlated to sowing density response.

The Spearman correlation analysis was performed on traits generated from all three tests, taking advantage of the non-destructive nature of image-based phenotyping, which enables the generation of traits' time series, instead of one-time-measurements. Traits, whose Spearman coefficients *r* had a *p*-value lower than 5 %, were considered correlated to either Br or Tr. In Test 1, there were 4 correlated traits with Br but none with Tr, which could be due to the poor phenotypic expression at this early growth stage (V4). The more developed the plants were, the more traits were identified. For instance, 7 Br-correlated traits were detected from Test 2, while 17 such traits were selected from Test 3. Similarly, Test 2 and 3 data generated 2 and 4 Tr-correlated traits, respectively (the results of Spearman tests from test 1–3 can be found in the supplementary file). The Br- and Tr-correlated traits from Test 3, which was chosen for further data analysis, are summarized in Fig. 5, where their mean Spearman coefficients, as well as their 95 % Confidence Interval (CI) are demonstrated. The detailed report of correlation between each trait and Br and Tr from each test is available in the supplemental document (Suppl. Table 3–8).

From the 17 Br-correlated traits, 5 with the highest absolute values of r ($r \geq 0.7$) were selected for further data analysis. These traits, together with the 4 Tr-correlated traits, are listed in Table 1 with brief descriptions of them that attempt to explain the biological meaning of these different traits.

Furthermore, Br as functions of 5 selected traits are plotted in Fig. 6, where the monotonic relationship between the traits with Br can be clearly seen. Such a relationship is also reflected by the Spearman coefficients of these pairs, which are all larger than 0.6. Similar observations can be made in Fig. 7, where Tr as functions of the 4 selected traits are displayed.

The 5 traits with the strongest correlation with Br were traits that corresponded to the morphological structure of plants., e.g., two traits of the voxel ratios and voxel_kurtosis, which describes the distribution of leaves along the stem, and %_hull_coverage which characterizes the positionning of leaves along the stem, for instance how overlapped and/or upright the leaves are. In contrast, the Tr-correlated traits were all related to the leaf orientation of the plants, i.e. the average leaf angle, leaf inclination, and the depth of light penetration, except one

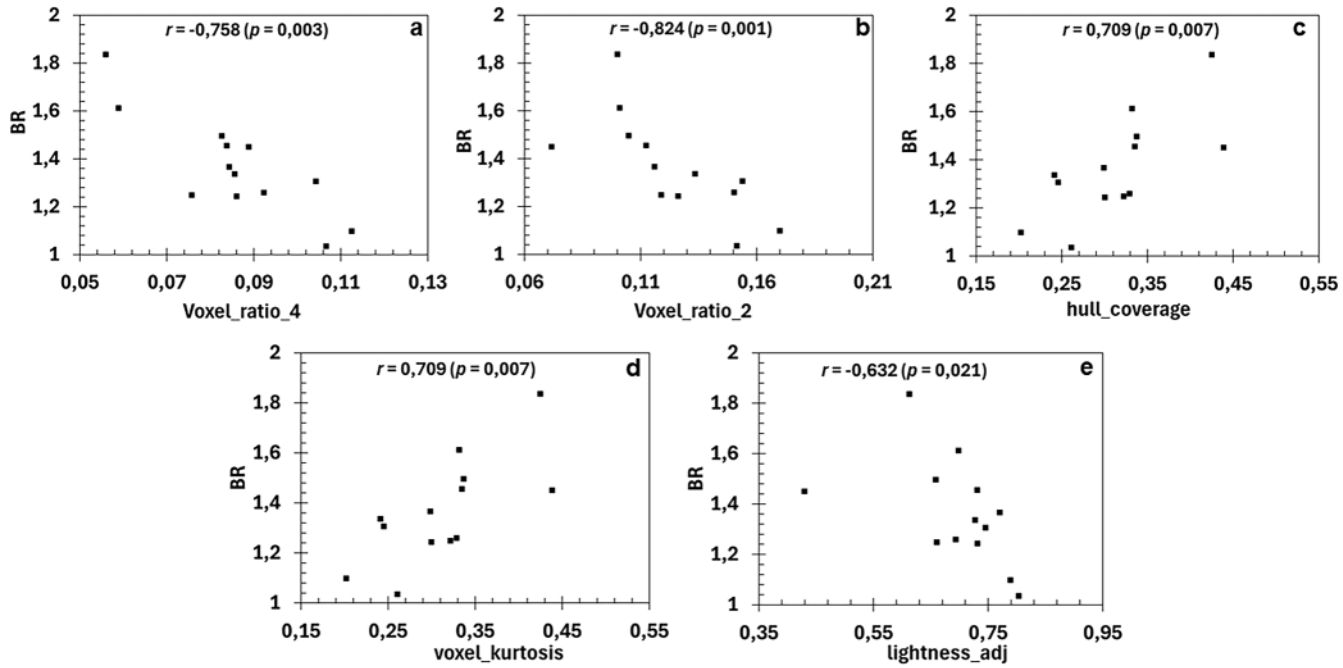

Fig. 6. Br as functions of correlated phenotypic traits: Voxel_ratio_4 (a), Voxel_ratio_2 (b), hull_coverage (c), voxel_kurtosis (d) and lightness_adj (e). For each pair, the spearman correlation coefficient r and its p-value is given.

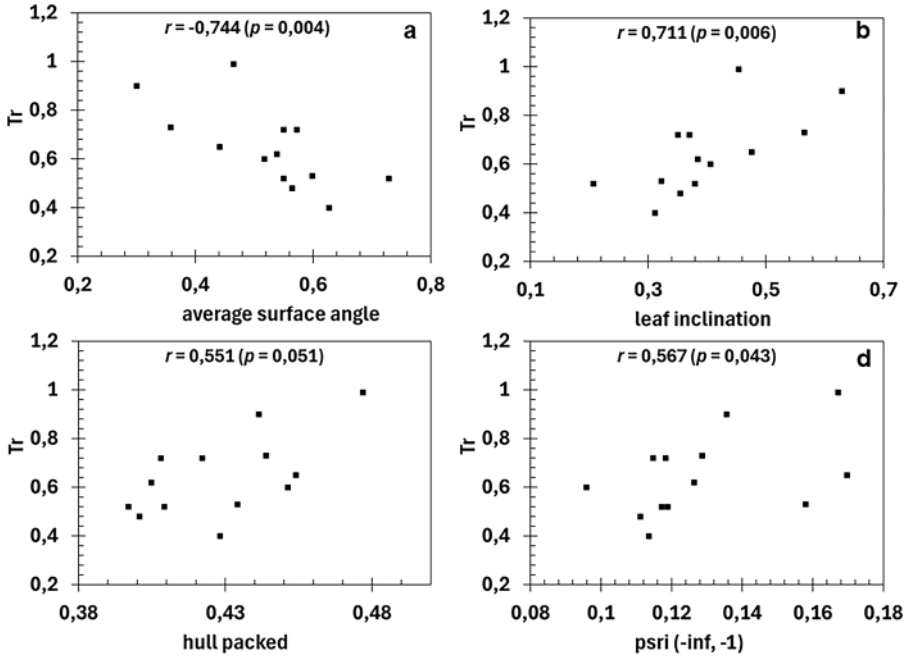

Fig. 7. Tr as functions of correlated phenotypic traits: average surface angle (a), leaf inclination (b), hue packed (c) and psri (-inf, −1) (d).

multispectral one. Take leaf_inclination as an example, it measures the average orientation of a plant's leaves by calculating the ratio of total leaf area against projected leaf area. In the case of horizontally aligned leaves, the total leaf area and the projected leaf area are the same and the ratio is 1. In the case of vertically aligned leaves, the total leaf area is higher than the projected area, so that the inclination values are higher than 1. These results are new in sorghum and are fully in line with similar results obtained earlier in maize [11], where the distribution of the leaf area along the vertical axis, and in particular phenotypes presenting a higher proportion of the leaf area on the lower part of the canopy had been selected over time and allowed a better light interception. Here, the added value from this work is that this better light interception also contributes to a better response to increasing planting density. In another review study, leaf erectness, thanks to higher leaf angle, was also associated to higher photosynthetic efficiency and yield, although this study did not look at the effect of these traits on the response to planting density [4]. Our findings also fully align with the theoretical description of a "smart canopy" ideotype in a previous theoretical review [8]. This ideotype would have some leaf area on the top of the canopy and most of it deep down in the canopy, which would ensure that all light is used and that a larger proportion of the leaf area is involved in photosynthetic activities. The consistency with earlier

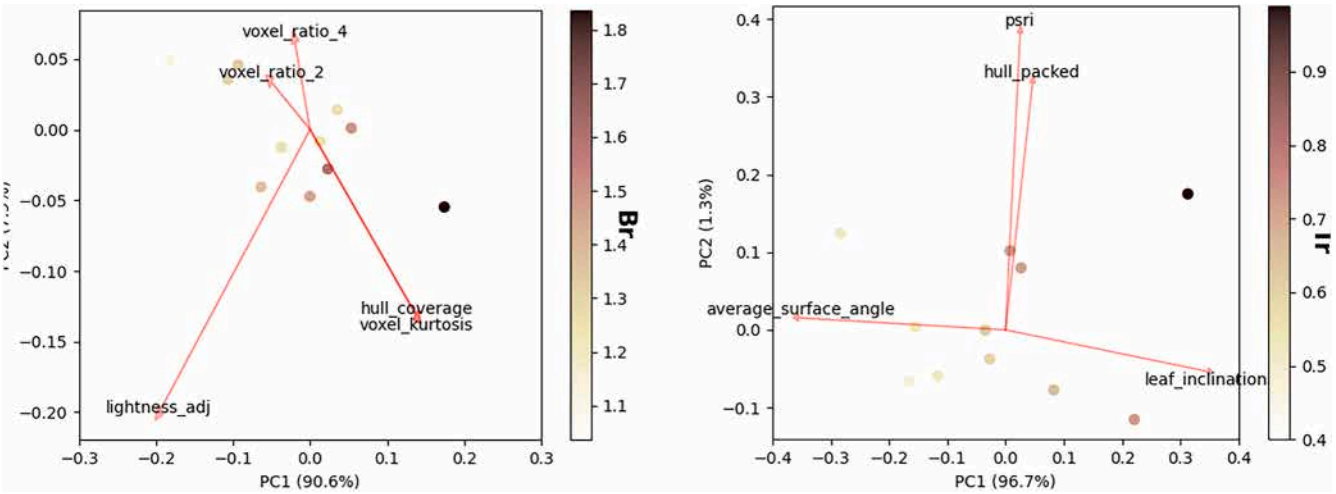

Fig. 8. PCA biplots of Br-correlated traits (left) and Tr-correlated traits (right). Each point on the biplots represent one genotype and its colour the corresponding Br or Tr value, respectively. Arrows demonstrate the alignment of each selected trait with PC1 and PC2 in the biplots (For details refer to Suppl. Table 9–10).

results in other species is exciting and opens to the possibility to breed for these traits. Future work would then be necessary to evaluate carefully the heritability of these traits, and to develop phenotyping tools and protocols to measure them in the field conditions. This will likely be a major, challenging but necessary effort, with various critical aspects to take into account, including trait interactions and effect of density on trait values.

3.5. Genotype discrimination

The selected Tr- and Br-correlated traits were further evaluated by PCA to explore the feasibility of separating genotypes of various sowing density responses (indicated by Br and Tr values), using the combination of selected traits. It should be first noticed that the first principal component (PC1) explained about 91 % of the variation in Br, and about 97 % of the variation for Tr. Future work will need to focus on generating similar data in a wider range of genotypes to allow for a more detailed description of contributing variables to the PC's. Genotypes are in the biplot with assigned colours corresponding to their Tr or Br values (see Fig. 8).

The results of the PCA analysis of Br from Test 2 and 3 showed a similar trend: the top 3 traits that had the most impact on PC1 and PC2 were the same, i.e., hull_coverage, voxel_kurtosis and lightness_adj, and the distribution of genotypes in the PC space were alike. The PC1 and PC2 scores were mainly determined by these top 3 features, since the loading vectors of the other features, namely voxel ratio 2 and 4, were relatively small (Fig.8, left). Moreover, it can be seen that the genotypes with a relatively larger Br are located on the lower right side of the biplot, which had high PC1 score and low PC2 score. A higher PC1 and a lower PC2 score are associated with a larger hull_coverage and voxel_kurtosis, which could represent genotypes with less leaf overlapping and/or more upright leaves that are not uniformly distributed along the stem, for instance a relatively larger portion of voxels in the lower part of the canopy, which is fully in line with the "smart canopy" ideotype that was theorized earlier (Fig. 3 in [8]). In other word, these are the plants with morphological structures allowing deeper light penetration, more complete light interception, and higher photosynthesis in the lower canopy.

Although not having as strong an association as hull_coverage and voxel_kurtosis, a lower lightness_adj was also partially linked with an increasing Br in Fig. 8 (left). Lightness_adj measures the relative depth of light penetration, by dividing the depth of light penetration by a plant's height. A smaller lightness_adj indicates less light penetration into the lower canopy, but it cannot be directly translated to less photosynthetic activities. For example, a smaller lightness_adj could indicate a plant with a bigger expanded top or middle portion, which does not facilitate deeper light penetration into the lower canopy. However, a bigger expanded top canopy could mean a larger leaf area is exposed to the light, and thus it could lead to more photosynthetic activities. Reversely, a higher lightness_adj could indicate a plant with narrow leaves allowing light penetration deep down but possibly with an incomplete light interception (hence less photosynthetic activities). Therefore, a comprehensive and accurate understanding of a plant can be achieved via the combination of multiple traits, rather than a single trait. In this case, the genotypes with relatively larger Br identify themselves with a morphological structure that favours better photosynthesis in the lower canopy, such as genotypes with less overlapped leaves and a relatively larger lower canopy.

The analysis of Tr was performed on selected traits from Test 3, not Test 2, because only 2 Tr-correlated traits were detected from Test 2, which was not sufficient for multivariable analysis. Furthermore, the loadings of each trait on PC1 and PC2 are displayed as arrows in the biplots, of which the directions and lengths represent the alignment of traits to PC1 and PC2. The results of the analysis suggested that genotypes with relatively larger Tr values tend to be located on the right side of the biplot, thus having relatively higher PC1 scores (see Fig. 8, right). PC1 score was mostly determined by smaller average_surface_angle and larger leaf_inclination as the influence of the other two traits are trivial. This indicated that the genotypes with larger Tr values differ from others by having more vertically aligned leaves. This aligns well with an earlier study [28] in which genotypes with larger Tr values had also higher WUE. It also alignes well with previous review or theoretical studies [4, 8] Genotypes with higher Tr values were interpreted to be those allowing more light to penetrate inside the canopy, leading to bottom leaves taking a larger share of the whole plant's photosynthesis. The leaf transpiration from the bottom leaves were indeed shown to explain the lower vapor pressure deficit (VPD) values inside the canopy, which then led to higher WUE [33].

3.6. ANOVA and post-hoc analysis

The selected traits, of which the mean values were used in the correlation study and PCA analysis, were also evaluated whether they show statistically significant genotypic variation. Such evaluation was performed via One-Way ANOVA using genotype as the factor and the within-genotype mean of each trait as the response. The analysis results show that genotype is a significant factor influencing all the selected traits (see details in the supplement document).

hull_coverage					voxel_kurtosis					lightness_adj					average_surface_angel							leaf_inclination						
geno	Grouping				geno	Grouping				geno	Grouping				geno	Grouping						geno	Grouping					
15	A				15	A				2	A				5	A						15	A					
20	A				20	A				4	A				12	A	B	C	D			16	A	B				
18	A	B			18	A	B			12	A	B			9	A	B	C	D	E		18	A	B	C			
16	A	B			16	A	B			8	A	B			19	A	B	C	D	E		7		B	C	D		
19	A	B	C		19	A	B	C		5	A	B			2	A	B	C	D	E		8		B	C	D	E	
7	A	B	C		7	A	B	C		16	A	B			20		B	C	D	E		6			C	D	E	F
6	A	B	C		6	A	B	C		9	A	B			4		B	C	D	E		20			C	D	E	F
5		B	C	D	5		B	C	D	19	A	B	C		6		B	C	D	E		4			C	D	E	F	G
12		B	C	D	12		B	C	D	7	A	B	C		8			C	D	E	F	2			C	D	E	F	G
2		B	C	D	2		B	C	D	6	A	B	C		7				D	E	F	G	19			C	D	E	F	G
8		B	C	D	8		B	C	D	18	A	B	C		18					E	F	G	9			C	D	E	F	G
9		B	C	D	9		B	C	D	20		B	C		16						F	G	12			C	D	E	F	G
4				D	4				D	15				D	15							G	5						G

Fig. 9. Demonstration of genotypic variations of hull_coverage, voxel_kurtosis, lightness_adj, average_surface_angel and leaf_inclination (from left to right). Genotypes that do not share a group letter are significantly different.

As part of the ANOVA evaluation, the normality and the homogeneity of variances of the data have been investigated. While majority of the data are normally distributed and have homogeneous variance, there exist some outliers from each feature (more so with lightness_adj than others). However, as these outliers are distributed in multiple genotypes, instead of from 1—2 specific ones, and one-way ANOVA is robust in dealing with slightly non-normal distribution data, it was decided not to remove any outliers from the analysis (for details please see Fig. S1 and S2 in the supplement document).

Additionally, a post-hoc Tukey analysis has been performed to identify which genotypes show significant differences in the selected traits. Fig.9 gives the example of the Br-correlated traits, where the 13 genotypes are clustered in different groups, based on their within-genotype mean values of the corresponding traits. The genotypes, who are not in the same group, are significantly different from each other for the corresponding traits.

The ANOVA result, including that from its post-hoc analysis, provides more certainty in the conclusions drawn from the previous data analysis study and also gives insights how future study can be focused on: to generate data from a bigger sample pool, with bigger sample size within genotypes and more diversity in genotypes. The analysis results strongly suggest that the selected features can be used to identify genotypes with positive response to sowing density and even potentially used as phenotypic-markers for the breeding of the high yield crops. A potential usage of this result can be that the same selected features for a new genotype with an unknown density response can be analysed with the same PCA approach to predict whether it belongs to the high-density response group. Such an approach can be used as a screening procedure for quick selection of promising candidates for further investigation.

4. Conclusions and recommendations

The present study has identified phenotypic traits, measured by 3D laser scanning, that are strongly correlated to two traits used as indicators of the degree of sowing density responses in sorghum genotypes. This is an important innovation because traits explaining important field-based agriculture productivity indicators could be pinpointed by high-tech tools – here 3D laser scanner and related algorithms - in distant environments. Our results strongly suggest that morphological traits favouring better photosynthesis in the lower canopy lead to a larger Biomass ratio (Br) under increased sowing density. On the other hand, a plant of more vertically aligned leaves tends to have larger Tr values, indicating more efficient water usage (high WUE) under increasing sowing density. Furthermore, the PCA analysis results show that the identified traits can be further developed as phenotypic-markers for the prediction of the density response behaviour for novel genotypes. Additionally, our research approach outlines a possible framework to integrate 3D-imaging into plant research. Future study will focus on screening more genotypes with bigger sample sizes to enrich the database, to bring more insights about the mechanisms behind genotypic variations in sorghum responses to sowing density, as well as to enable the construction of statistical models for sowing density response predictions. Future studies also implies developing phenotyping tools and protocols for measuring these traits under field conditions.

Ethical statement

Authors declare they have not used AI to prepare this manuscript

CRediT authorship contribution statement

Wenli Xue: Writing – original draft, Software, Methodology, Investigation, Formal analysis, Data curation. **Ewaut Kissel:** Writing – review & editing, Supervision, Software, Methodology, Conceptualization. **András Tóth:** Writing – review & editing, Methodology, Conceptualization. **Raphael Pilloni:** Writing – review & editing, Methodology, Investigation, Conceptualization. **Vincent Vadez:** Writing – review & editing, Supervision, Resources, Project administration, Methodology, Investigation, Funding acquisition, Conceptualization.

Declaration of competing interest

The authors declare that they have no known competing financial interests or personal relationships that could have appeared to influence the present study.

Acknowledgements

Senior and last authors were supported by the Make Our Planet Great Again (MOPGA) ICARUS project (Improve Crops in Arid Regions and future climates) funded by the Agence Nationale de la Recherche (ANR grant ANR-17-MPGA-0011), by the Occitanie Region through a financial contribution to grant ANR-17-MPGA-0011, and by Montpellier University of Excellence (I-Site MUSE). WX and VV are also thankful to expert technical help from Daniel Moukouanga and Pierre Serin from IRD.

Supplementary materials

Supplementary material associated with this article can be found, in the online version, at doi:10.1016/j.atech.2024.100756.

Data availability

Data will be available on request.

References

[1] A.H. Mesfin, F. Girma, Understanding sorghum farming system and its implication for future research strategies in humid agro-ecologies in Western Ethiopia, J. Agricult. Food Res. 10 (2022) 100456.
[2] R. Tanwar, et al., Nutritional, phytochemical and functional potential of sorghum: a review, Food Chem. Adv. 3 (2023) 100501.
[3] R. Pilloni, et al., The genotypic variation in the positive response of sorghum to higher sowing density is linked to an increase in water use efficiency, Eur. J. Agron. 158 (2024) 127207.
[4] M.B. Mantilla-Perez, M.G. Salas Fernandez, Differential manipulation of leaf angle throughout the canopy: current status and prospects, J. Exp. Bot. 68 (21–22) (2017) 5699–5717.
[5] D.J. Timlin, et al., Plant Density and Leaf Area Index Effects on the Distribution of Light Transmittance to the Soil Surface in Maize, Agron J. 106 (5) (2014) 1828–1837.
[6] A.J. Burgess, et al., Exploring Relationships between Canopy Architecture, Light Distribution, and Photosynthesis in Contrasting Rice Genotypes Using 3D Canopy Reconstruction, Front Plant Sci. 8 (2017).
[7] X.G. Zhu, S.P. Long, D.R. Ort, What is the maximum efficiency with which photosynthesis can convert solar energy into biomass? Curr. Opin. Biotechnol. 19 (2008) 153–159.
[8] D.R. Ort, S.S. Merchant, J. Alric, A. Barkan, R.E. Blankenship, R. Bock, Redesigning photosynthesis to sustainably meet global food and bioenergy demand, in: Proceedings of the National Academy of Sciences, USA 112, 2015, pp. 8529–8536.
[9] L. Cabrera-Bosquet, C. Fournier, N. Brichet, C. Welcker, B. Suard, F. Tardieu, High-throughput estimation of incident light, light interception and radiation-use efficiency of thousands of plants in a phenotyping platform, New Phytolo. 212 (2016) 269–281.
[10] S.K. Truong, R.F. McCormick, W.L. Rooney, J.E. Mullet, Harnessing genetic variation in leaf angle to increase productivity of sorghum bicolor, Genetics 201 (2015) 1229–1238, https://doi.org/10.1534/genetics.115.178608.
[11] R.P.A. Perez, et al., Changes in the vertical distribution of leaf area enhanced light interception efficiency in maize over generations of selection, Plant Cell Environ. 42 (7) (2019) 2105–2119.
[12] T.R. Gregory, Artificial Selection and Domestication: modern Lessons from Darwin's Enduring Analogy, Evolution 2 (1) (2009) 5–27.
[13] H. Tao, et al., Proximal and remote sensing in plant phenomics: 20 years of progress, challenges, and perspectives, Plant Commun. 3 (6) (2022) 100344.
[14] H.O. Awika, et al., Developing Growth-Associated Molecular Markers Via High-Throughput Phenotyping in Spinach, Plant Genome 12 (2019).
[15] Q. Xiao, et al., Advanced high-throughput plant phenotyping techniques for genome-wide association studies: a review, J. Adv. Res. 35 (2022) 215–230.
[16] Y. Huang, et al., Agricultural remote sensing big data: management and applications, J. Integr. Agric. 17 (9) (2018) 1915–1931.
[17] I. Azpiroz, et al., Comparison of Climate Reanalysis and Remote-Sensing Data for Predicting Olive Phenology through, Machine-Learning Methods. Remote. Sens. 13 (2021) 1224.
[18] D. Dodig, et al., Image-derived traits related to mid-season growth performance of maize under nitrogen and water stress, Front Plant Sci. 10 (2019).
[19] D. Eyland, et al., High-throughput phenotyping reveals differential transpiration behaviour within the banana wild relatives highlighting diversity in drought tolerance, Plant Cell Environ. 45 (6) (2022) 1647–1663.
[20] A. Paturkar, G.Sen Gupta, D.G. Bailey, Plant trait measurement in 3D for growth monitoring, Plant Methods 18 (2022).
[21] M.M. Rahaman, et al., Advanced phenotyping and phenotype data analysis for the study of plant growth and development, Front Plant Sci. 6 (2015).
[22] R.Q.Y. Wang, Y. Zhou, Z. Liang, J.C. Schnable, A High-Throughput Phenotyping Pipeline for Image Processing and Functional Growth Curve Analysis, Plant Phenomics (2020).
[23] W. Hu, et al., Nondestructive 3D image analysis pipeline to extract rice grain traits using x-ray computed tomography, Plant Phenomics 2020 (2020).
[24] F.P. Boogaard, E.J. van Henten, G. Kootstra, The added value of 3D point clouds for digital plant phenotyping – A case study on internode length measurements in cucumber, Biosyst. Eng. 234 (2023) 1–12.
[25] S. Das Choudhury, et al., Leveraging Image Analysis to Compute 3D Plant Phenotypes Based on Voxel-Grid Plant Reconstruction, Front Plant Sci. 11 (2020).
[26] Zang, J., et al., Field-measured canopy height may not be as accurate and heritable as believed – Evidence from advanced 3D sensing. 2022.
[27] J.A. Jimenez-Berni, et al., High Throughput Determination of Plant Height, Ground Cover, and Above-Ground Biomass in Wheat with LiDAR, Front Plant Sci. 9 (2018).
[28] R. Pilloni. Agronomical and physiological study of the response of sorghum and pearl millet crops to higher sowing density in the semi-arid tropics. PhD thesis, Univ. Montpellier, 2022. https://theses.hal.science/tel-04087443v1/file/PILLONI_2022_archivage.pdf.
[29] V. Vadez, S. Choudhary, J. Kholova, C.T. Hash, R. Srivastava, A. Ashok Kumar, A. Prandavada, M. Anjaiah, Transpiration efficiency: insights from comparisons of C4 cereal species, J. Exp. Bot. 72 (2021) 5221–5234, https://doi.org/10.1093/jxb/erab251.
[30] V. Vadez, J. Kholova, S. Medina, A. Kakkera, H. Anderberg, Transpiration efficiency: New insights into an old story, J. Exp. Bot. 65 (2014) 6141–6153, https://doi.org/10.1093/jxb/eru040.
[31] Zotarelli, L., et al. Step by Step Calculation of the Penman-Monteith Evapotranspiration (FAO-56 Method) 1. 2015.
[32] Allan, R., L. Pereira, and M. Smith, Crop evapotranspiration-Guidelines for computing crop water requirements-FAO Irrigation and drainage paper 56. Vol. 56. 1998.
[33] R. Pilloni, A. Faye, A. Kakkera, J. Kholova, R. Badji, C. Faye, V. Vadez, Higher sowing density of pearl millet increases productivity and water use efficiency in high evaporative demand seasons, Front. Plant Sci. 13 (2022) 1035181, https://doi.org/10.3389/fpls.2022.1035181.